

# Morphology and Properties of Blends with Different Thermoplastic Polyurethanes and Polyolefines

PETRA PÖTSCHKE,<sup>1</sup> KATRIN WALLHEINKE,<sup>1</sup> HOLGER FRITSCHKE,<sup>1</sup> HERBERT STUTZ<sup>2</sup>

<sup>1</sup> Institut für Polymerforschung Dresden e.V., Hohe Straße 6, D-01069 Dresden, Germany

<sup>2</sup> BASF AG, Kunststofflaboratorium, D-67056 Ludwigshafen, Germany

Received 31 July 1996; accepted 24 October 1996

**ABSTRACT:** Unmodified blends of two thermoplastic polyurethanes (TPU) and six polyolefines were used to study the influence of the component viscosities on the blend morphology and mechanical properties. Blends were produced by melt mixing using a twin screw extruder. Interactions between the blend components could not be detected by DSC, DMA, selective extraction, and SEM micrographs of cryofractures. The variation in tensile strength with blend composition produce a U-shaped curve with the minimum between 40 and 60 wt % of polyolefine. At similar viscosity ratios ( $\eta_d/\eta_m$ ), blends with polyether based TPU (TPU-eth) have a finer morphology than blends with polyester based TPU (TPU-est). This is due to the lower surface free energy of the polyether soft segments compared to the polyester soft segments. Different morphologies also lead to changes in mechanical behavior. Blends with TPU-eth show a lower decrease in tensile strength with blend composition than blends with TPU-est. The viscosity ratio between TPU and polyolefines can be directly correlated to the blend morphology obtained under similar blending conditions. TPU/PE blends show a lower dispersity than TPU/PP blends, due to the higher viscosity ratios of TPU/PE blends. This results in a greater reduction in tensile strength with the disperse phase content.

© 1997 John Wiley & Sons, Inc. *J Appl Polym Sci* **64**: 749–762, 1997

**Key words:** thermoplastic polyurethanes; polyolefines; viscosity ratio; blend morphology; mechanical properties

## INTRODUCTION

Blends of thermoplastic polyurethanes (TPU) and polyolefines (PO) are highly incompatible because of large differences in polarities and high interfacial tensions. This immiscible polymer system was used to determine the influence of the viscosity ratio on the blend morphology, the morphology stability, and the mechanical properties. The viscosity ratio was varied by using six polyolefines with different viscosities. The stability of the mor-

phologies of the extruded blends was determined by comparison with the morphologies of injection-molded specimens. The influence of the chemical structure of TPU (polyester and polyether-based polyurethanes) on the morphologies of their blends was also investigated.

The dispersity in melt mixed immiscible blends is influenced by material parameters like viscosity and polarity ratios, blend composition, and processing conditions.<sup>1–4</sup> The mechanisms governing morphology development are drop breakup and coalescence.<sup>5</sup> While drop breakup is not dependent on the content of the disperse phase,<sup>6</sup> coalescence is strongly influenced by the blend composition.<sup>3,7–9</sup>

Assuming newtonic material behavior and sim-

Correspondence to: Petra Pötschke.

Contract grant sponsor: Bundesministerium für Bildung, Wissenschaft, Forschung und Technologie.

© 1997 John Wiley & Sons, Inc. CCC 0021-8995/97/040749-14

ple shear flow, drop breakup occurs when the shear forces deforming the droplet are higher than the interfacial forces. From this balance, Taylor<sup>6</sup> obtained a relation for the maximum stable drop [eq. (1)]. As coalescence is not included in this relation, the Taylor-diameter ( $d_T$ ) can be used as a value for the lower limit of the particle size (Taylor-limit).

$$d_T = \frac{4\gamma_{1,2}(\lambda + 1)}{\dot{\gamma}\eta_m(19\lambda/4 + 4)} \quad (1)$$

with

- $d_T$  = drop diameter according to Taylor
- $\gamma_{1,2}$  = interfacial free energy
- $\lambda$  = viscosity ratio =  $\eta_d/\eta_m$
- $\eta_d$  = viscosity of disperse phase
- $\eta_m$  = matrix phase viscosity
- $\dot{\gamma}$  = shear rate

The influence of the viscosity ratio on the morphology of melt mixed blends has been discussed by several authors for different blend systems. Wu<sup>4</sup> used polyamide/rubber blends and observed that the smallest particles are generated when the viscosities of the components are similar ( $\lambda = 1$ ). The viscosities and interfacial tensions of the blend components, which were varied over a wide range, were correlated with the final particle diameter [ $d_{wu}$ , Wu-diameter, eq. (2)]:

$$d_{wu} = \frac{4\gamma_{1,2}\lambda^{\pm 0.84}}{\dot{\gamma}\eta_m} \quad (2)$$

with exponent = +0.84 for  $\lambda > 1$  and -0.84 for  $\lambda < 1$ .

The concentration of the disperse phase was 15 wt %, and the shear rate was  $100 \text{ s}^{-1}$ . Serpe et al.<sup>10</sup> further developed this equation by substituting the matrix viscosity by the blend viscosity and by introducing a term that considers the composition and, thus, coalescence effects. Using this modified Weber number, Serpe confirmed Wu's equation for the blend system PE/PA6. Mixing conditions, blend composition, and components were varied.

Using different polypropylenes as matrix polymers, Hietaoja et al.<sup>11</sup> found a linear increase in the particle size with increasing viscosity ratio for polyamide 66/polypropylene blends. In contrast, no correlation between particle size and viscosity ratio was found when using PP as dispersed

phase. Favis and Chalifoux<sup>12,13</sup> investigated polypropylene/polycarbonate blends and observed an increase in the particle size for viscosity ratios below 1, which are obtained with polypropylenes as matrix component. A minimum value was observed at a viscosity ratio of 0.15 in blends with polypropylenes as the dispersed phases.

The results from these investigations do not always agree due to differences in the content of the dispersed phases, mixing technologies, particle size measurements methods, and shear rates selected for the calculation of the viscosity ratios.

The phase size increases and the size distribution broadens significantly at higher dispersed phase contents. This is caused by coalescence, which has been previously observed at concentrations lower than 1%.<sup>7</sup> Favis and Willis<sup>9</sup> report that the particle size/composition relation did not significantly depend on the viscosity ratio and interfacial tension. A master curve for eight different polymer pairs mixed in an internal mixer was obtained by shifting the data along the volume fraction axis. The shift factor depends on the viscosity and interfacial properties. Heikens et al.<sup>14</sup> found a dependence of the increase in particle size with the content of disperse phase on the overall viscosity of the polymer system. Blends of PE dispersed in PS showed a higher increase in the particle size with composition than blends of PS in PE. This asymmetric behavior can be explained by a decrease in blend viscosity in PS-based blends with rising PE content. As a result, the equilibrium between breakup and coalescence is shifted more in the direction of coalescence than in PE-based blends. Tokita<sup>8</sup> showed a dependence of the particle size/composition relation on the viscosity of the dispersed phase. In NR/EPM blends, the increase with composition is more pronounced if the viscosity of the dispersed phase is low. Roland and Böhm<sup>15</sup> and Gisbergen<sup>16</sup> found that an increase in the viscosity of the dispersed phase also inhibits coalescence. Min et al.<sup>17</sup> found a dependence of the particle size on the content of the dispersed phase in PE/PS blends, but variation of the viscosity ratio by use of three different polyethylenes showed not a systematic influence. Everaert<sup>18</sup> describe for PP/(PS/PPO) blends an enhanced droplet breakup with decreasing of viscosity ratio achieved by higher PPO content in the miscible phase PS/PPO. This results in lower droplet sizes and a reduced coalescence of dispersed PP droplets.

The processing conditions play an important role in morphology development during melt mix-

ing, especially at higher concentrations of the dispersed phase and at high viscosity ratios. Favis and Therrien<sup>19</sup> found that the phase size of 5% PC in PP was four times higher in an internal mixer than in a twin-screw extruder at a viscosity ratio of 17.3. At low viscosity ratios, the difference between the morphologies is not significant. The morphologies of PC/PP blends with 5% of PP and viscosity ratios below 0.22 were not sensitive to the screw speed and output. According to Plochcki,<sup>20</sup> the particle size as a function of mixing energy goes through a minimum, caused by the different influences of the mixing conditions on the processes of dispersion and coalescence.

The mechanical properties of blends are reported to be morphology dependent. This effect is usually discussed using blends where the reduction of the particle size is achieved by compatibilization. This leads to the problem that not only the particle size, but also the composition and interfacial free energy and, thus, the phase adhesion are influenced. There are no publications dealing with the dependence of the mechanical properties on both the viscosity ratio and blend composition. The influence of the particle size on the impact strength was investigated by Wu,<sup>21</sup> who found a dramatic increase in Izod impact strength in PA6/rubber blends at a critical particle size.

## EXPERIMENTAL

### Materials and Their Characterization

The POs used in these investigations were commercial products of BASF AG, Germany. The TPUs were provided by Elastogran GmbH, Germany. Some properties of the materials are shown in Table I.

The viscosities of the blend components were measured using a high-pressure capillary rheometer Rheograph 2003 (Göttfert, Germany) with a capillary die of 1 mm and a L/D ratio of 30. The measured values were corrected using the Rabinowitsch–Weissenberg correction and fitted using the Carreau-model. The viscosity ratio of the blend components was determined by division of the viscosity functions of the dispersed phase and the matrix polymer.

The surface free energy of the polymer melts was determined using the pendant drop analysis.<sup>22,23</sup>

### Blend Preparation

The TPU was dried under vacuum for 3 h at 100°C before processing.

Blends were extruded with a corotating, intermeshing twin screw extruder ZSK 30 (Werner and Pfleiderer, Germany) with a screw configuration adapted to the blend system. The following conditions were used: screw speed 150 r.p.m., output 10 kg/h, melt temperature 230°C (TPU-est) or 210°C (TPU-eth). The residence time was about 50 s, the torque between 50 and 95%.

Injection molding was done using an Arburg 221E/221P (Arburg, Germany) to produce specimens for the tensile test according to DIN 53455 (specimen S3 with a thickness of 4 mm). The residence time in the molten state was up to 5 min at a melt temperature of 230 or 210°C, respectively. The injection pressure was about 70 bar, and the cycle time 30 s.

For some of the investigations with PE 1 and PP 1, a Battenfeld 500/200 machine (Battenfeld, Germany) was used to produce specimens S2 for the tensile test according to DIN 53504 for elastomers. The processing conditions were the same as above. The specimens were tested after annealing for 24 h at 100°C.

### Morphology

The particle size of the blends was determined using light microscopy (BH 2, Olympus, Germany) on cryomicrotomed thin sections in phase contrast. The thickness of the thin sections was 3  $\mu\text{m}$ . The microscope was either furnished with a camera for photographs or with a CCD camera for digitalization of the images for quantitative analysis. The pictures were acquired under comparable conditions (brightness, contrast) and analyzed with a Quantimet 970 (Leica, Germany) using a programmed algorithm. Manual corrections were minimized to secure comparability of the results.

The distribution of the equivalent circle diameter was measured. The mean particle diameter and the standard deviation as a measure for the broadness of particle size distribution are used for interpretation. At least 1000 particles were analyzed for each blend morphology.

Injection-molded S2 tension test specimens were cryofractured within their gage length. The fractures were analyzed using a low-voltage SEM (GEMINI, Zeiss Oberkochen, Germany) without previous sputtering at an acceleration voltage of 1 kV.

**Table I Properties of Materials**

Denotation	Material		Surface	Viscosity at		Viscosity Ratio at 200 s <sup>-1</sup>	
			Tension (mN/m)	200 s <sup>-1</sup> (Pas)		$\eta_{PO}/\eta_{TPU-eth}$	$\eta_{PO}/\eta_{TPU-est}$
			230°C	210°C	230°C	210°C	230°C
	Thermoplastic polyurethane elastomers (TPU)						
TPU-est	Elastollan® C 64D	based on polyesterdiol	29.4 <sup>a</sup>		791		
TPU-eth	Elastollan® 1195A	based on polyetherdiol	22.8 <sup>a</sup>	748			
	Polyolefines (PO)						
	Polyethylenes (PE)						
PE 1	Lupolen® 4261A	high density polyethylene	<sup>b</sup>	1454	1293	1.95	1.64
PE 2	Lupolen® 5021D	high density polyethylene	<sup>b</sup>	990	880	1.32	1.11
PE 3	Lupolen® 1810D	low density polyethylene	<sup>b</sup>	643	547	0.86	0.69
	Polypropylenes (PP)						
PP 1	Novolen® 1127 MX	homopolymer	19.4	234	221	0.31	0.28
PP 2	Novolen® 2600 LX	block copolymer	<sup>b</sup>	287	275	0.38	0.35
PP 3	Novolen® 1127 N	homopolymer		216	180	0.29	0.23

<sup>a</sup> Measured on model substances for soft segments.

<sup>b</sup> Not measurable by pdA.

## RESULTS AND DISCUSSION

### Rheological Properties of the Blend Components and Interfacial Free Energy

As the dependence of viscosity on the shear rate is less pronounced for TPU than for polyolefines, the viscosity ratios are not constant with the shear rate. PE 1 has a higher viscosity than TPU; for PE 2 and PE 3, this is the case only at low shear rates. All of the polypropylenes have a lower viscosity than TPU. Figures 1 and 2 show the viscosity functions of polyolefines and TPU-est at 230°C and the resulting viscosity ratios as function of shear rate. For the shear rate of 200 s<sup>-1</sup>, the viscosities and the viscosity ratios for the POs and both TPUs are shown in Table I.

Due to the similar rheological behavior of the two TPUs at their processing temperatures and the slight differences in the value for PO viscosities at these temperatures, the viscosity functions and the viscosity ratios for TPU-eth (curves not shown) are comparable to those of TPU-est.

Direct measurements or calculations of the interfacial free energy (or interfacial tension) between TPU and the other blend components were either not successful or not practicable.

As a result of the microphase separation of

TPU-soft segments (SS) and TPU-hard segments (HS) both inside the bulk and at the interface during the preparation of the test specimens,<sup>24,25</sup> contact angle measurements on solid surfaces did not lead to reliable results. This was confirmed by measurements that showed no differences in the surface free energy and polarity of the two TPUs.

A direct measurement of the interfacial free energy in melts using the pendant drop method was not possible because of the insufficient thermal stability of the TPU melt. Therefore, two low molecular weight model substances for the TPU-SS were used to determine the temperature dependence of the surface free energy. These values were compared with those of PP 1 as an example for nonpolar polyolefines. The polyether-based SS have a lower surface free energy than the polyester based SS, and the value for PP is lower than that of the TPU-SS (Table I). The differences in surface free energies of TPU-SS and PP are about 3 mN/m for SS-eth and about 10 mN/m for SS-est over the whole range of the temperatures used.

### Interactions in This Blend System?

Incompatibility was found in other TPU blend systems, for example, with ABS, ASA, PS,<sup>26,27</sup>

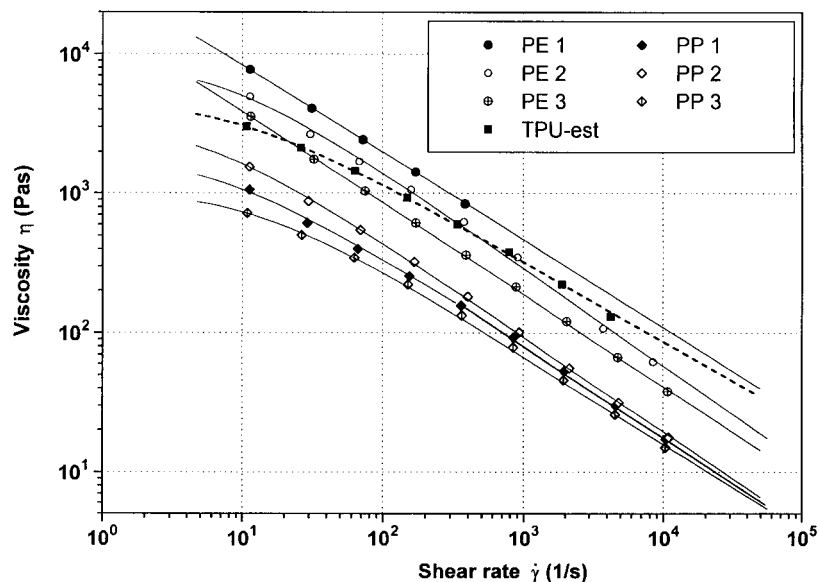


**Figure 1** Viscosity functions of TPU-est and polyolefines at 230°C.

PA6,<sup>28,29</sup> PVDF,<sup>30</sup> and EVA.<sup>31</sup> It was shown that the second blend component can change the microphase separation of the TPU, if interactions, especially with the hard segments, take place.<sup>31–34</sup> Miscibility of TPU and PVC<sup>35</sup> and EVA<sup>28</sup> was observed in some investigations.

The differences in surface free energies and polarities of TPU and PO suggested an incompatibility. The investigations of Tang et al.<sup>36</sup> confirmed this assumption.

Low-voltage SEM on unspattered cryofractured specimens (Fig. 3) revealed no sign of interfacial adhesion.

Dynamic mechanical analysis (Fig. 4) showed that the glass transition temperatures of both components in these blends were not influenced by the blend partner. The microphase separation within the TPU was not changed significantly.

Differential scanning calorimetry (DSC, Fig. 5) indicated that the melt enthalpies of the components and their characteristic melting temperatures are not influenced by blending.

Figure 6 shows that a complete separation of blends into their components was achieved by selective extraction in dimethylformamide (DMF) after 24 h at room temperature.

### Morphology of Blend Granules

The morphologies of the TPU-est/PO blends get coarser with a rising viscosity ratio between the

blend components (Fig. 7). The three polypropylenes have low viscosity ratios in the range of 0.23 to 0.35, resulting in similar morphologies with a fine dispersion of PP within the TPU matrix. The blends with polyethylene have higher viscosity ratios; with TPU-est and PE1 blends having the largest particles. The viscosity ratio between these components is 1.64.

This relation between particle size and viscosity ratio becomes even more obvious from the results of the quantitative analysis of the particle size (Fig. 8). An increasing viscosity ratio results in a linear rise in the number-average mean particle diameter and a broadening of the particle size distribution (shown as standard deviation).

Figure 9 shows an example for the blend morphologies achieved by using polyether–polyurethane instead of polyester–polyurethane. The blend of TPU-eth and PE1 has the highest viscosity ratio of all polymer blends used. In spite of this, the particle size is much smaller than in the TPU-est and PE1 blend (compare Figs. 7 and 8). The particle size is the same order of magnitude as in the TPU-est and PP blends, but a quantitative analysis of the morphology was not practicable. The dispersion of the polyolefine was much finer in all of the TPU-eth blends than the corresponding TPU-est blends. This is accounted for by the fact that the surface free energy of the polyether soft segment is lower than that of the poly-

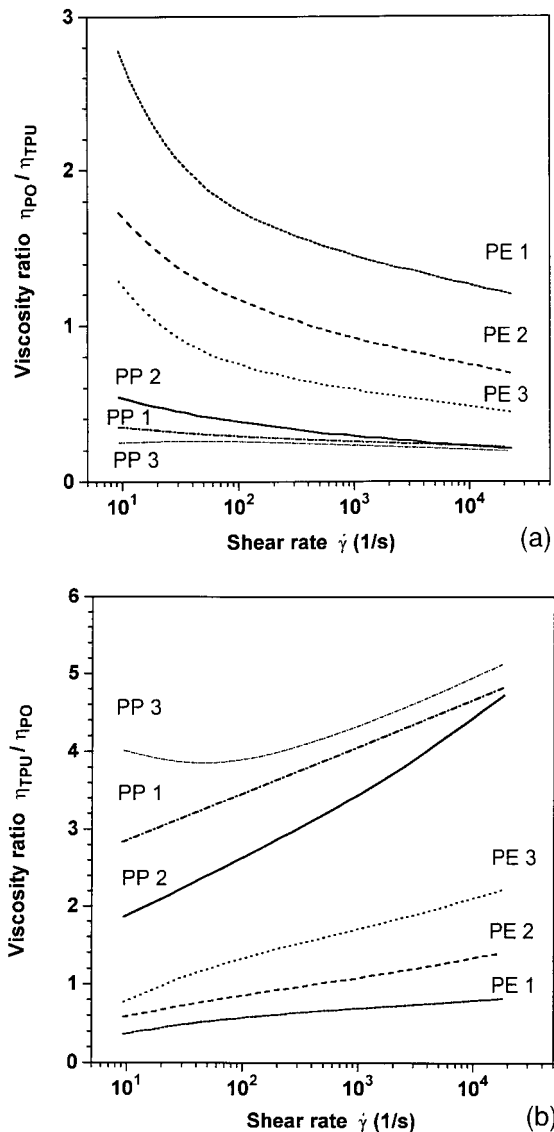


**Figure 2** Viscosity ratio  $\lambda$  between TPU-est and polyolefines at 230°C for (a) TPU as matrix component; (b) TPU as dispersed phase.

ter soft segment and, consequently, closer to that of the nonpolar polyolefines.

### Coarsening of the Morphology during Injection Molding

The blend granules were injection molded to specimens under comparable conditions for all blend systems.

The morphology of these samples is shown in Figure 7 (TPU-est). The dependence of the mean particle size and particle size distribution on the viscosity ratio is even more pronounced than in

the blend granules (Fig. 8). This observation was confirmed for TPU-eth by SEM on cryofractures (Fig. 3). The difference in the particle sizes of blends with PP 1 ( $\lambda = 0.31$ ) and PE1 ( $\lambda = 1.95$ ) is obvious.

In addition, it can be seen (Figs. 7 and 8) that an increasing viscosity ratio not only induces larger particle sizes but also produces a more pronounced coarsening during processing. In blends with PP, distinct differences in particle size between granules and injection-molded specimens were not found. In contrast, there is a large effect in the blends with PE, especially when using PE 1 as blend component.

This effect was quantified by defining the degree of coarsening as the quotient of the mean particle size in the injection-molded specimens and in the granules. Figure 10 shows the linear increase in this quotient with the viscosity ratio.

In contrast to melt mixing results, coalescence seems to predominate drop breakup during injection molding. In the several steps of the injection-molding process, the melt is kept at low shear rates, which allows coalescence to take place.

In the blend system used, two factors favor coalescence of dispersed particles with a high viscosity. At first, the large particles generated during melt mixing (high viscosity ratios) have a higher probability of collision.<sup>7</sup> In addition, the deformation of two colliding drops is lower at higher dispersed phase viscosities (Fig. 11). Due to of the resulting smaller area of the matrix film between the particles and the higher forces transferred by the droplets, the removal of the interlaying film is facilitated by higher dispersed phase viscosities. Schoolenberg<sup>38</sup> also reports that two droplets in a lower viscous matrix coalesce faster when the viscosity of the drops is higher. She investigated coalescence between two drops with a fixed radius using a spinning drop apparatus.

### Comparison with Taylor-Limit and Wu-Diameter

Using eqs. (1) and (2) the particle diameters in the blend system polyolefines as dispersed phase and TPU-est as matrix were calculated and compared to the particle diameters measured in blend granules (Fig. 12). According to Heidemeier,<sup>37</sup> the shear rate in a twin screw extruder ZSK 30 at the selected screw speed is between  $50 \text{ s}^{-1}$  in the conveying element and  $5000 \text{ s}^{-1}$  in the kneading elements, which were used in our investigations. These two values were selected for the calculation. A mean shear rate for the blending pro-

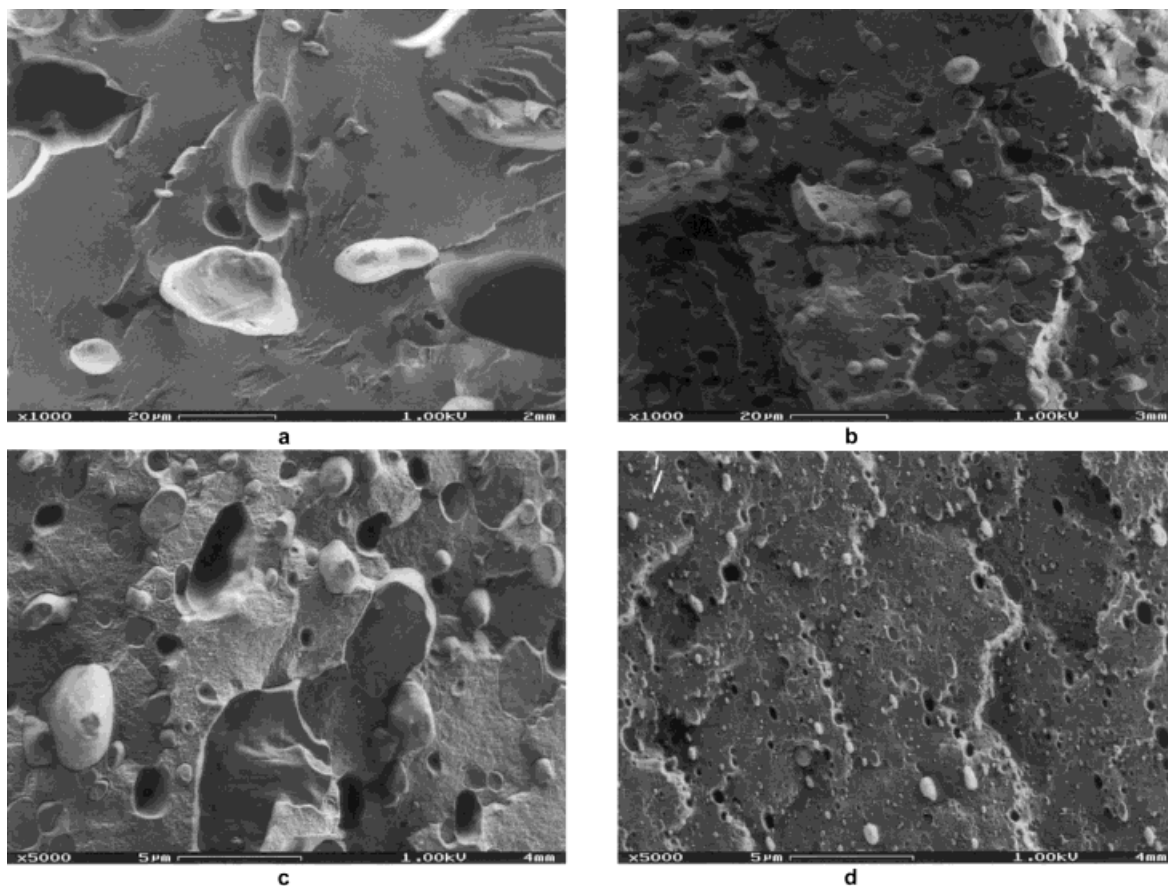


**Figure 3** SEM micrographs of cryofractures of TPU/PO = 80/20 blends (a) TPU-est/PE1; (b) TPU-eth/PE1; (c) TPU-est/PP1; (d) TPU-eth/PP1.

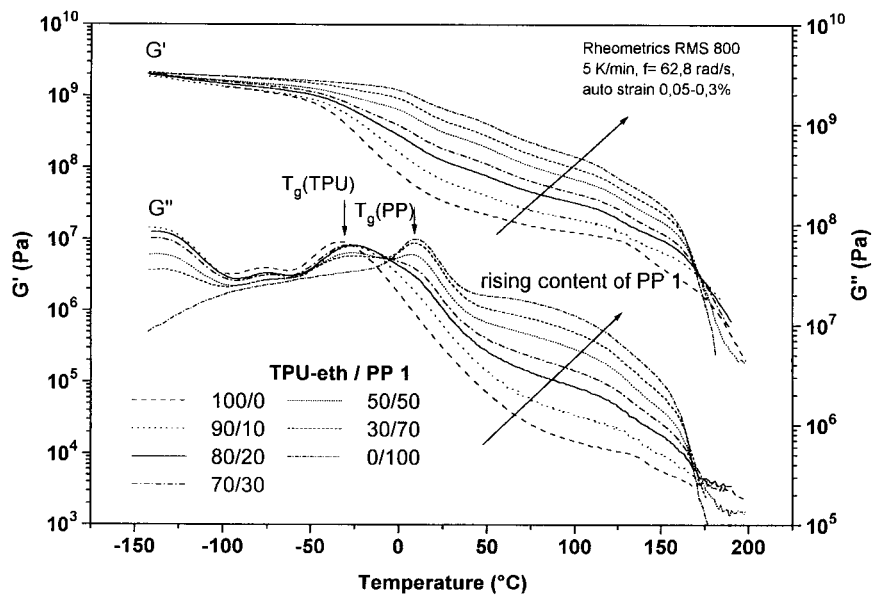


**Figure 4** Storage moduli  $G'$  and loss moduli  $G''$  vs. temperature for TPU-eth/PP1.

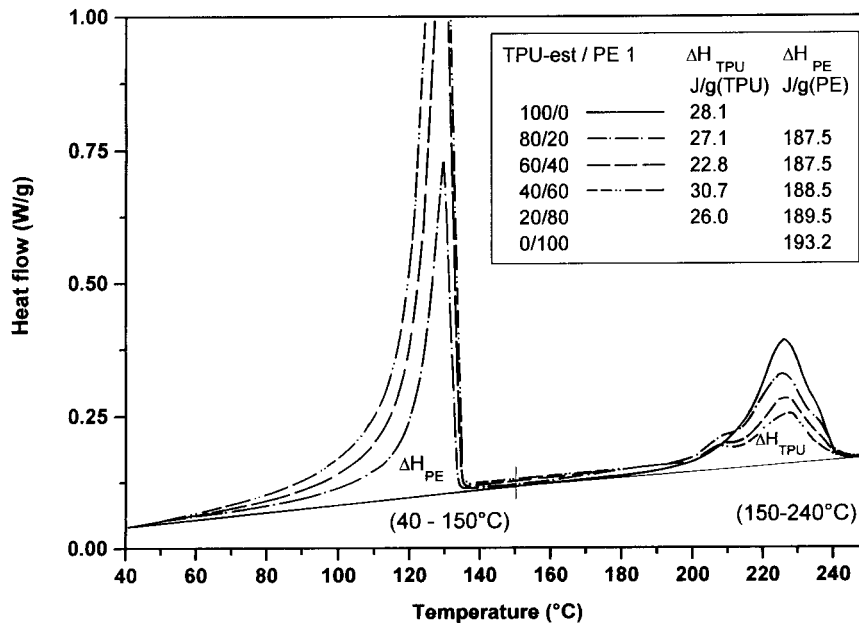


**Figure 5** DSC thermograms for different compositions of TPU-est/PE1 blends (first heat, 10 K/min).

cess of  $200 \text{ s}^{-1}$  was chosen, as recommended in refs. 11 and 37. For the interfacial free energy  $\gamma_{1,2}$  a value of 10 mN/m for the combination TPU-est/PO was assumed (Table I).

Application of the Taylor eq. (1) reveals no influence of the viscosity ratio on the particle size. The reason for this is that the most important factors, interfacial free energy and matrix viscosity, are constant in the blend system used. The calculated particle diameters are much lower

than the measured ones. This can be explained by the fact that Taylor does not consider coalescence, which is pronounced in these blends due to the high dispersed phase content (20%).

Application of Wu's eq. (2) gives diameters that are 10-fold higher than the ones obtained by Taylor's equation. These values are also higher than the measured ones; only in the region of a low viscosity ratio and a shear rate of  $50 \text{ s}^{-1}$  is the Wu-diameter comparable to the measured particle diameters. A linear increase in the mean particle size with rising viscosity ratio, as observed in this study, is predicted by Wu for  $\lambda > 1$  only. The minimum in the particle size at a viscosity ratio of 1, as implied in the Wu-equation, was not confirmed by our measurements.

This indicates that coalescence plays an important role not only during the injection molding of these blends but also during the development of the blend morphology in twin screw extruders. It can be assumed that the differences in coalescence rate in injection molding also are responsible for the different particle sizes in melt mixed blends.

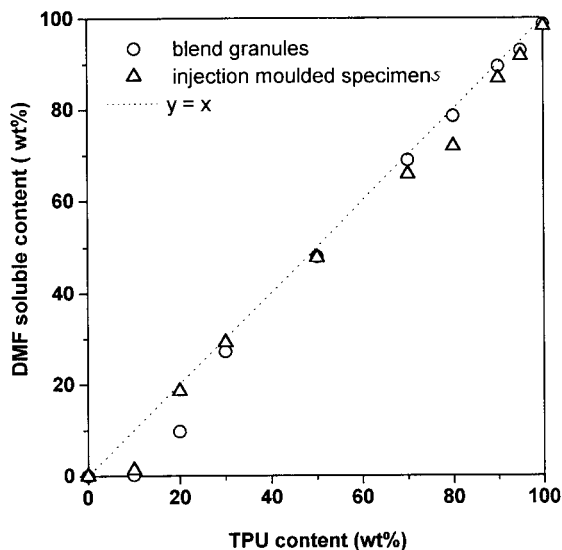


**Figure 6** Solubility of TPU-eth/PE1 blends in DMF.

## Mechanical Properties of Blends

### Stress-Strain Behavior

TPU shows the typical behavior of an elastomer with a continuous increase in stress and strain



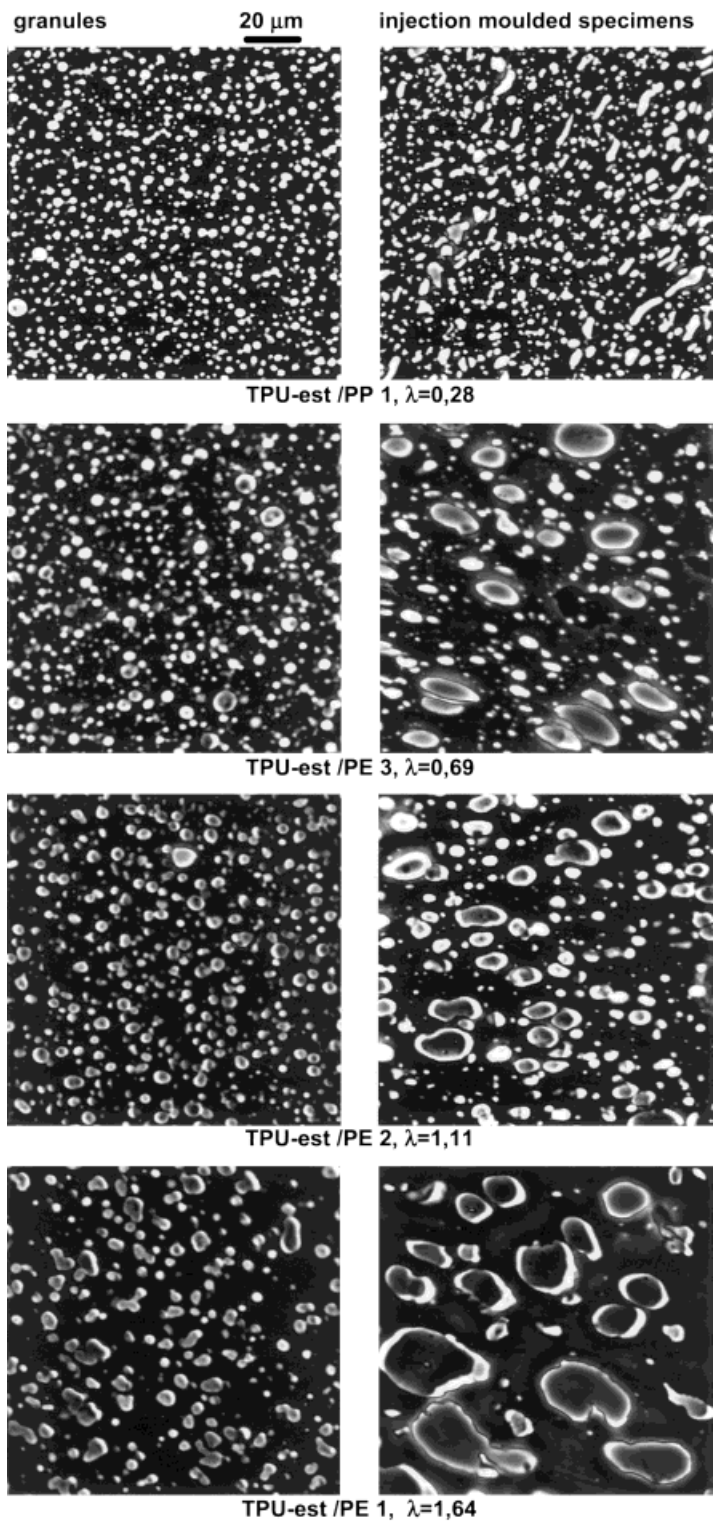


**Figure 7** Light micrographs of TPU-est/PO = 80/20 blend granules and injection-moulded samples with different viscosity ratios  $\lambda$  (at  $\dot{\gamma} = 200 \text{ s}^{-1}$ ).

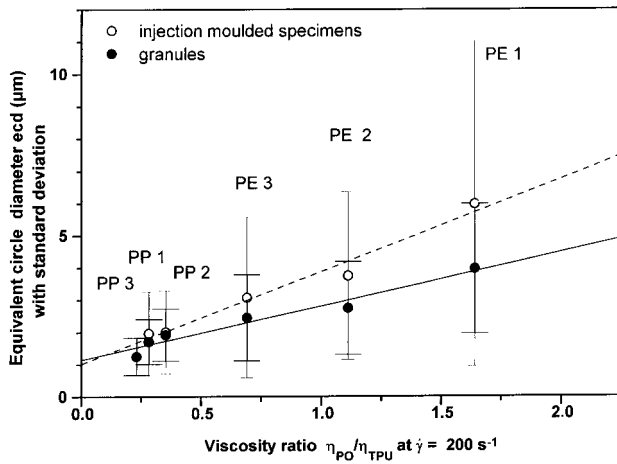


**Figure 8** Mean particle size in of TPU-est/PO = 80/20 blend granules and injection-molded specimens

up to break. Polyolefines have a higher yielding stress than stress at break (Fig. 13). With up to the addition of 30–40 wt % polyolefines in TPU, the composition at which phase inversion occurs, the typical behavior of TPU is predominant. As soon as PO becomes the matrix, the stress–strain curve changes significantly, and the elongation at break is reduced to values below the ones of the pure PO. The behavior of TPU-eth is comparable to that of TPU-est. As a result of the lower content of hard segments in TPU-eth, the tensile strength is lower and the elongation at break is higher than that of TPU-est. The low elongation at break of the polyolefines is due to test speed used (DIN 53504 for elastomers).

#### Composition Dependence of Tensile Strength

All blends show a U-shaped curve for the dependence of the tensile strength on the blend composi-

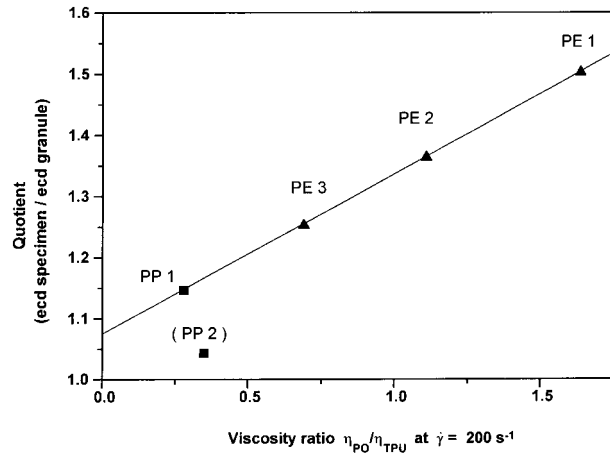


**Figure 10** Coarsening of blend morphology during injection molding for TPU-est/PO = 80/20 blends.

tion (Fig. 14). This is in agreement with studies by Deanin<sup>39</sup> of blends of TPU with 10 different polymers. All incompatible blends show this typical U-shaped curve. Previous investigations showed a decrease in tensile strength with the addition of a second polymer.<sup>31,33</sup> The extent of the reduction in properties is related to the blend morphology, with blends having a finer dispersity showing less reduction in properties. In order to be able to compare the tensile strength of blends with the tensile strengths of the pure components, the deviation from the theoretical mixing rule was introduced. The principle is shown in Figure 14. The results are plotted versus the content of PO in Figure 15.

Blends with TPU-est show a larger decrease in tensile properties with the content of disperse phase than blends with TPU-eth. The reduction in properties is less pronounced in blends with PP

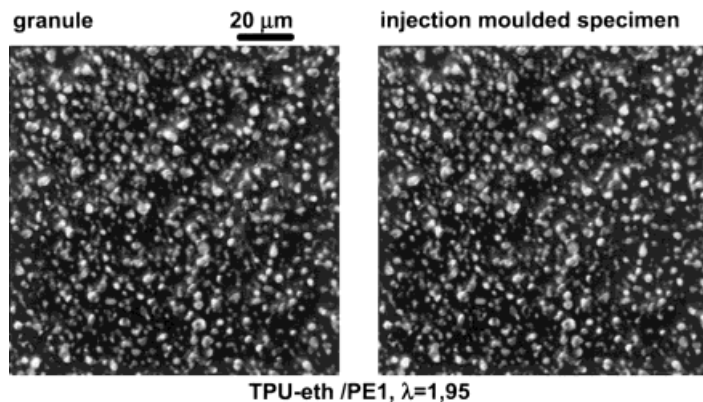


**Figure 9** Light microscopy micrographs of TPU-eth/PE1 = 80/20 blend granule and injection-molded specimen.

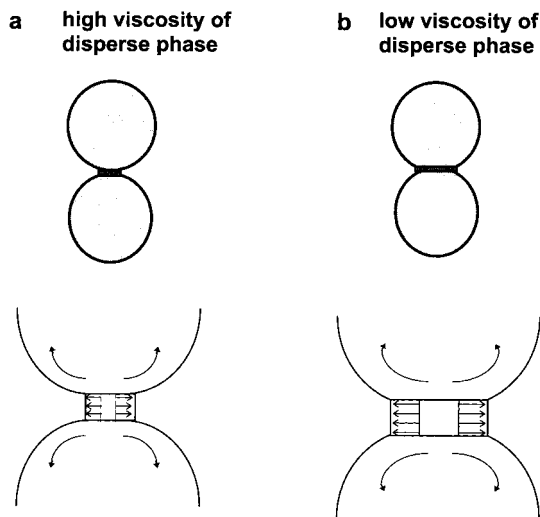


**Figure 11** Area of liquid interfacial films consisting of matrix polymer between two deformable, colliding drops for (a) high viscous and (b) low viscous drops (the viscosity of the matrix and the mobility of the interphases are constant).

than in blends with PE. At low PO concentrations (up to 20 wt %), blends with TPU-eth show a slight increase in tensile strength, possibly caused by a small change in the microphase separation within the TPU (indication is given by DMA, see Fig. 5). This behavior has been reported in earlier studies.<sup>31,33</sup>

The elongation at break (Fig. 14) decreases with the PO-content, and phase inversion occurs at 40%. Only with TPU-eth/PP 1, the system with the finest dispersity and the lowest decrease in tensile strength, is phase inversion shifted to 60 wt % PP.

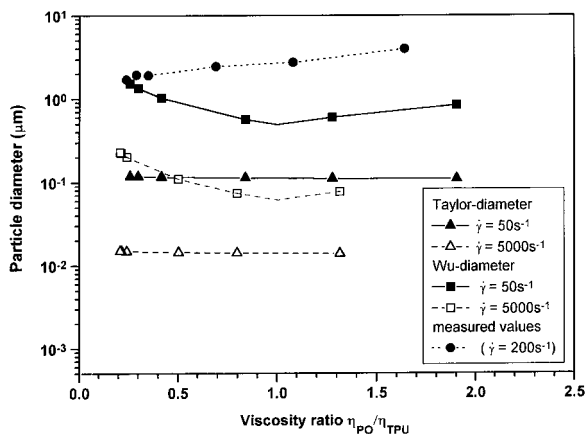


**Figure 12** Theoretical and measured particle sizes in TPU-est/PO blends.

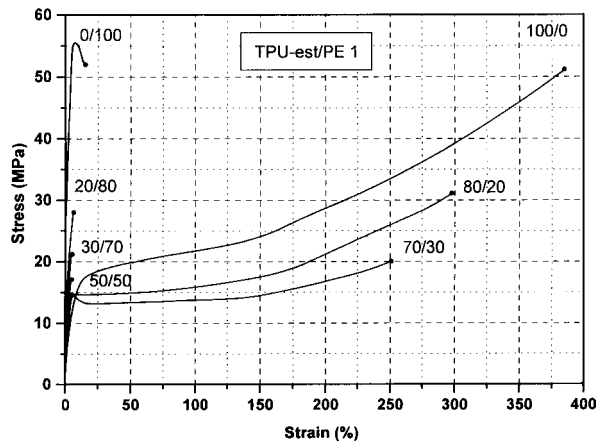


**Figure 13** Stress–strain curves for different compositions of TPU-est/PE1 blends (tensile test, S2-specimens, 200 mm/min).

The dependence of the tensile strength on the composition of blends consisting of both TPUs and three different polyethylenes is shown in Figure 16. Blends with TPU-eth show a lower decrease of the tensile strength with composition, as can clearly be seen in the blends with PE 1 and PE 3. The differences in the tensile strengths of the different combinations are higher with TPU as matrix. No direct correlation to the viscosity ratio was to be found.

**SUMMARY AND CONCLUSION**

In the blend system thermoplastic polyurethanes/polyolefines interactions between the blend components cannot be detected by DSC, DMA, selective extraction, and SEM. The tensile strength of compositions shows a U-shaped curve with a minimum between 40 and 60 wt % polyolefine.

In general, at similar viscosity ratios ( $\eta_d/\eta_m$ ), blends with polyether-based TPU have a finer dispersed morphology than blends with polyester-based TPU. This is due to the lower differences in surface free energies of the polyether soft segments and PO compared to the polyester soft segments and PO. The viscosity ratio between TPU and polyolefines can be correlated directly to the blend morphology obtained under similar blending conditions. The mean equivalent circle diameter measured in TPU-est/PO blends with 20 wt % polyolefine was between 1.7 and 6  $\mu\text{m}$ .

The observed increase in the particle size with the viscosity ratio is higher than that reported for PP/PC<sup>12</sup> but lower than found for PP/PA6.<sup>4</sup> This

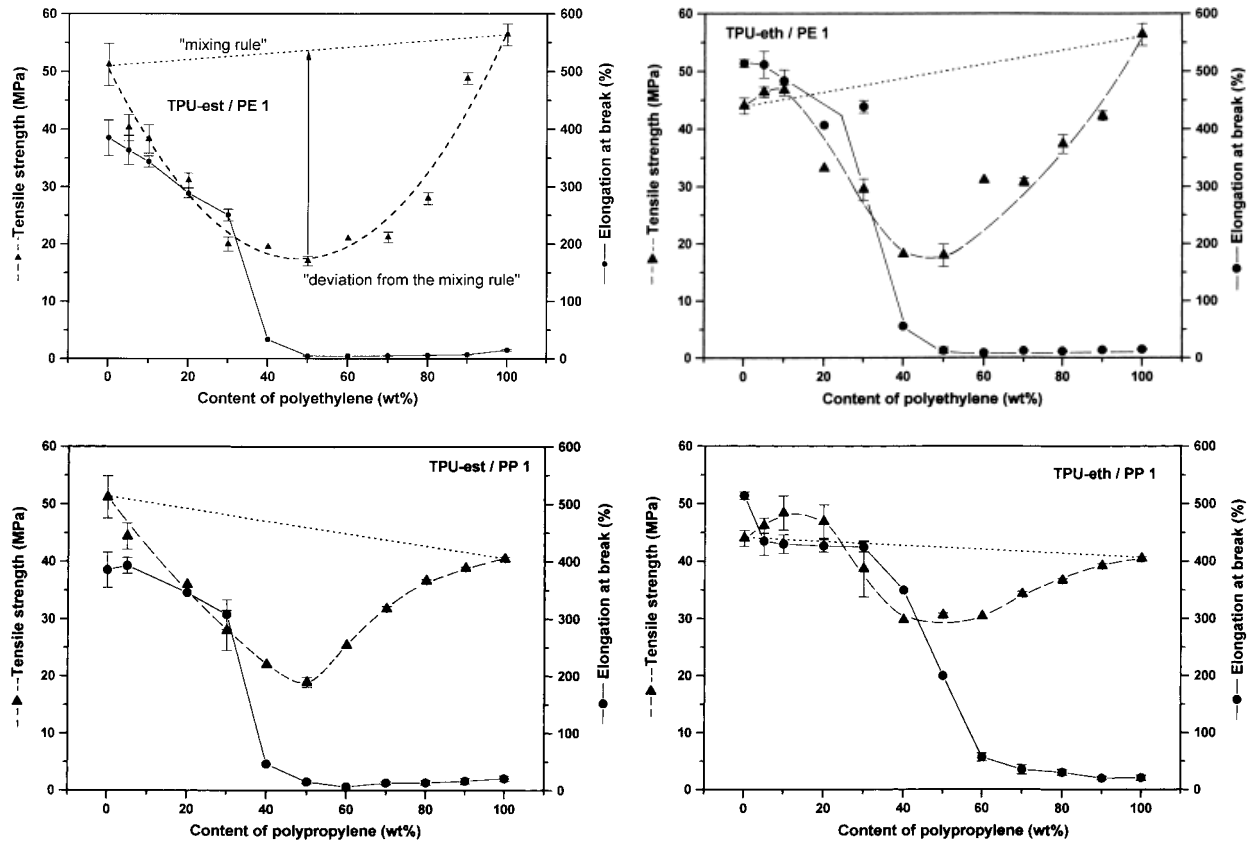


**Figure 14** Tensile strength and elongation at break vs. polyolefine content for different blend compositions (S2-specimens, 200 mm/min).

results from the different interfacial properties and blending technologies used.

A minimum in particle size at a viscosity ratio of 1, as reported by Wu<sup>4</sup> for polyamide/rubber systems was not observed. Interestingly, with polyethylene blends, a higher viscosity ratio in-

duces not only a higher particle size, but also results in an increased coarsening during injection molding. This indicates that coalescence plays an important role in the development of blend mor-

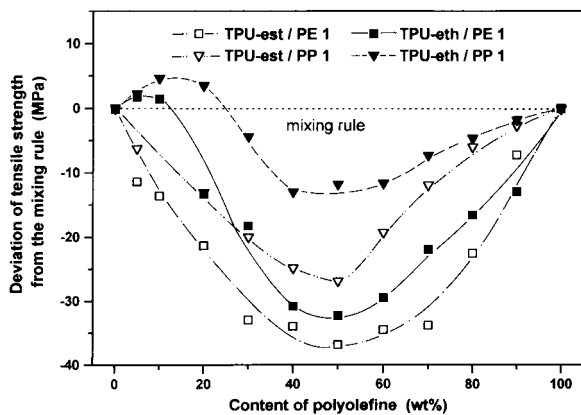


**Figure 15** Deviation of the tensile strength from the mixing rule for different blend compositions (S2-specimens, 200 mm/min), calculated from Figure 14.

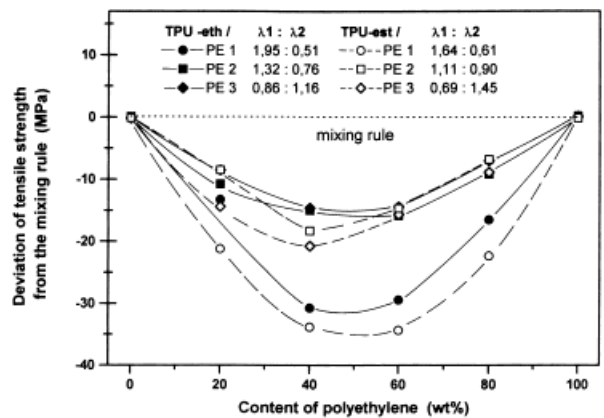


**Figure 16** Deviation of the tensile strength from the mixing rule for blends with different polyethylenes (S3-specimens, 50 mm/min); ( $\lambda_1 = \eta_{PE} / \eta_{TPU}$ ,  $\lambda_2 = \eta_{TPU} / \eta_{PE}$  at  $\dot{\gamma} = 200 \text{ s}^{-1}$ ).

phology during injection molding as well as during melt mixing.

In general, blends with TPU-est show a stronger decrease in tensile with disperse phase content, compared to blends with TPU-eth. Blends with PP show a smaller drop in properties, compared to blends with PE.

It can be concluded that the good mechanical properties of TPU can be preserved in blends with polyolefines by generating a finely dispersed morphology. This can be achieved by using components with similar surface free energies and low viscosity ratios.

Another possibility to improve the dispersity is given by compatibilization. In compatibilized blends, the interfacial free energy is reduced, phase adhesion is induced, and the morphology is stabilized against coalescence. This leads to an improvement of the mechanical properties of the polymer system.

Investigations into the compatibilization of the blend system TPU/PO are in progress; first results are discussed in refs. 40–42.

We thank the Bundesministerium für Bildung, Wissenschaft, Forschung und Technologie for its support of this work within the project 03M4077, "Phase stabilization in blends with highly incompatible polymers, especially thermoplastic elastomers." We are grateful for the help provided by Dr. Pionteck in supplying us with the pendant drop analysis.

## REFERENCES

1. E. H. Meijer and J. M. H. Janssen, in *Mixing and Compounding of Polymers*, I. I. Manas-Sloczower and Z. Tadmor, Eds., Hanser Publishers, Munich, New York, 1994.
2. K. Søndergaard and J. Lyngaae-Jørgensen, *Shear Flow-Induced Structural Changes in Polymer Blends and Alloys, Rheophysics of Multiphase Polymer Systems*, Technomic Publishing, Lancaster, 1995.
3. U. Sundararaj and C. W. Macosko, *Macromolecules*, **28**, 2647 (1995).
4. S. Wu, *Polym. Eng. Sci.*, **27**, 335 (1987).
5. L. A. Utracki and Z. H. Shi, *Polym. Eng. Sci.*, **32**, 1824 (1992).
6. G. I. Taylor, *Proc. R. Soc. Lond.*, **A138**, 41 (1932); **A146**, 501 (1934).
7. J. J. Elmendorp and A. K. Van Der Vegt, *Polym. Eng. Sci.*, **26**, 1332 (1986).
8. N. Tokita, *Rubber Chem. Technol.*, **50**, 292 (1977).
9. B. D. Favis and J. M. Willis, *J. Polym. Sci., Part B: Polym. Phys.*, **28**, 2259 (1990).

10. G. Serpe, J. Jarrin, and F. Dawans, *Polym. Eng. Sci.*, **30**, 553 (1990).
11. P. T. Hietaoja, R. M. Holsti-Miettinen, J. V. Sepälä, and O. T. Ikkala, *J. Appl. Polym. Sci.*, **54**, 1613 (1994).
12. B. D. Favis and J. P. Chalifoux, *Polym. Eng. Sci.*, **27**, 1591 (1987).
13. B. D. Favis and J. P. Chalifoux, *Polymer*, **29**, 1761 (1988).
14. D. Heikens, N. Hoen, W. Barentsen, P. Piet, and H. Ladan, *J. Polym. Sci., Polym. Symp.*, **62**, 309 (1978).
15. C. M. Roland and G. G. A. Böhm, *J. Polym. Sci., Polym. Phys. Ed.*, **22**, 79 (1984).
16. J. G. M. van Gisbergen and H. E. H. Meijer, *J. Rheol.*, **35**, 63 (1991).
17. K. Min, J. L. White, and J. F. Fellers, *Polym. Eng. Sci.*, **24**, 1227 (1984).
18. V. Everaert and G. Groeninckx, European Symposium on Polymer Blends, Maastricht, The Netherlands, 12–15 May 1996, Extended Abstracts, 111.
19. B. D. Favis and D. Therrien, *Polymer*, **32**, 1474 (1991).
20. Plochocki, S. S. Dagli, and R. D. Andrews, *Polym. Eng. Sci.*, **30**, 741 (1990).
21. S. Wu, *Polymer*, **26**, 1855 (1985).
22. M. Uzman, P. Pötschke, B. Song, and J. Springer, poster, Bayreuth Polymer & Research Symposium, 1993, book of abstracts, 70–72, Bayreuth 1993.
23. M. Uzman, J. Pionteck, P. Pötschke, B. Song, and J. Springer, MacroAkron '94, 35th IUPAC International Symposium on Macromolecules, Akron, OH, USA, 10.-5.07.1994, book of abstracts 1086.
24. C. S. Paik Sung and C. B. Hu, *Adv. Chem. Ser.*, **176**, 69 (1979).
25. J.-H. Chen and E. Ruckenstein, *J. Colloid Interface Sci.*, **135**, 476 (1990).
26. G. Demma, E. Martuscelli, A. Zanetti, and M. Zorzetto, *J. Mater. Sci.*, **18**, 89 (1983).
27. H. J. Radusch, R. Hendrich, G. H. Michler, and I. Naumann, *Angew. Makromol. Chem.*, **194**, 159 (1992).
28. J. T. Haponiuk, Investigations on Properties and Structure of Thermoplastic Polyurethane Blends, 3rd International Symposium on Thermoplastic Elastomers, 24.5.–26.5.1994.
29. C. Franke, P. Pötschke, M. Rätzsch, G. Pompe, K. Sahre, D. Voigt, and A. Janke, *Angew. Makromol. Chem.*, **206**, 21 (1993).
30. M. Z. Yue and K. S. Chian, *J. Appl. Polym. Sci.*, **60**, 597 (1996).
31. U. Mierau and M. Rätzsch, *Plaste Kautschuk*, **39**, 364 (1992).
32. M. Rätzsch, G. Haudel, G. Pompe, and E. J. Meyer, *Macrom. Sci. Chem.*, **A27**, 1631 (1990).
33. M. Rätzsch, J. Pionteck, and T. Rische, *Makromol. Chem., Macromol. Symp.*, **501**, 203 (1991).
34. J. Pionteck, P. Pötschke, T. Rische, and G. Pompe,

- Book of Abstracts 1028, Vortrag, MacroAkron '94, 35th IUPAC International Symposium on Macromolecules, Akron, OH, USA, 10.-15.07.1994.
35. F. Xiao, D. Shen, X. Zhang, Sh. Hu, and M. Xu., *Polymer*, **28**, 2335 (1987).
  36. T. Tang, X. Jing, and B. J. Huang, *Macromol. Sci.-Phys.*, **B33**, 287 (1994).
  37. P. K. H. Heidemeyer, Dissertation TH Aachen (Nr. D82), 46ff. (1990).
  38. T. E. Schoolenberg, F. Doring, and G. Ingenbleek, *Macromol. Symp.*, to appear.
  39. R. Deanin, St. Driscoll, and J. Krowchun, *Org. Coat. Plast. Chem.*, **40**, 664 (1979).
  40. K. Wallheinke, P. Pötschke, and H. Stutz, *J. Appl. Polym. Sci.*, to appear.
  41. P. Pötschke, H. Stutz, U. Mierau, and H. Fritsche, Poster, PPS European Regional Meeting 1994, Strasbourg, France, 29.-31.8.1994, book of abstract.
  42. P. Pötschke, K. Wallheinke, and H. Stutz, poster P23, The Polymer Processing Society, PPS European Regional Meeting 1995, Stuttgart, Germany, 26.-28.9.1995, book of abstracts